

CHRONIC reductions in cerebral blood flow associated with aging and progressive neurodegenerative disorders can precipitate cognitive failure. To assess whether chronic cerebrovascular insufficiency elicits neuronal apoptosis, apoptotic cell death in the hippocampus was quantitated in a rat model of permanent carotid occlusion. Bilateral carotid artery occlusion (2VO) was shown to induce apoptotic morphology and DNA strand breaks in hippocampal neurons 2 and 27 weeks after ligation. The rate of pyramidal cell apoptosis was higher at chronic (27 weeks) compared to sub-chronic (2 weeks) time points. 2VO-induced apoptosis resulted in a decrease in total pyramidal cell number at 27 weeks but not at earlier time points, indicating progressive neuronal loss. Working and reference memory errors in the radial arm maze were strongly correlated with the number of apoptotic neurons in CA1 but not CA3 pyramidal cell fields. These data provide the first indication that apoptotic loss of pyramidal neurons may play a role in memory impairment associated with clinical conditions of chronic cerebrovascular insufficiency.

**Key words:** Aging; Apoptosis; Hypoperfusion; Ischemia

## Chronic cerebral hypoperfusion elicits neuronal apoptosis and behavioral impairment

Steffany A. L. Bennett,<sup>CA,1,2</sup>  
Martin Tenniswood,<sup>2</sup>  
Jia-Hua Chen,<sup>1</sup>  
Christopher M. Davidson,<sup>1</sup>  
Marilyn T. Keyes,<sup>1</sup> Teresa Fortin<sup>1</sup>  
and Bruce A. Pappas<sup>1</sup>

<sup>1</sup>Institute of Neuroscience, Life Sciences Research Center, Carleton University, 1125 Colonel By Drive, Ottawa, Ontario, K1S 5B6, Canada; <sup>2</sup>W. Alton Jones Cell Science Center, 10 Old Barn Road, Lake Placid, NY 12946, USA

<sup>CA,1</sup>Corresponding Author and Address

### Introduction

Chronic disruption of cerebral blood flow resulting from carotid insufficiency and other ischemic states associated with aging can induce neurological deficits and dementia.<sup>1–4</sup> These conditions are exacerbated during Alzheimer's disease (AD) by cerebral amyloid angiopathy and morphological aberrations in brain microvasculature.<sup>5</sup> Circulation-dependent behavioral deficits can be modeled in experimental paradigms of chronic cerebrovascular insufficiency.<sup>4,6–8</sup> In rodents, permanent ligation of the common carotid arteries or two vessel occlusion (2VO) induces morphological abnormalities in hippocampal cells and quantifiable cell loss within 7 months of blood flow reduction.<sup>6,8</sup> Hippocampal atrophy correlates with impairment on visuospatial memory tasks.<sup>6–8</sup>

The mechanism by which pyramidal neurons are damaged during chronic hypoperfusion is not known. To assess whether cell death following 2VO is apoptotic (and thus potentially regulatable), we characterized the phenotype of dying neurons at early and late time points after surgery. Apoptosis is characterized morphologically by cell shrinkage, cytosolic blebbing, chromatin condensation, intranucleosomal DNA fragmentation, nuclear blebbing and nuclear

fragmentation into smaller apoptotic bodies.<sup>9,10</sup> Cell death is a multi-step process requiring one or more triggering stimuli to elicit expression of genes required for morphological change (pre-condensation phase). These apoptosis-associated transcripts code for proteins that mediate the loss of interaction between dying and surviving cells through degradation of the extracellular matrix and reduction of cytoplasmic volume (cytoplasmic condensation phase), the endonuclease-dependent DNA fragmentation and marginalization of the nucleosomal fragments to the nuclear periphery (nuclear condensation phase), the subdivision of dying cells into multiple apoptotic bodies (fragmentation phase), and the endocytosis and lysosomal degradation of apoptotic bodies by neighbouring cells or by activated phagocytes (phagocytosis phase).<sup>11</sup> Here we report that sustained cerebral hypoperfusion elicits apoptosis in CA1 and CA3 neurons and that the degree of programmed cell death correlates with the severity of behavioral impairment. These data provide the first indication that incremental apoptotic loss of pyramidal neurons may underlie progressive neurodegeneration associated with clinical conditions of chronic cerebrovascular insufficiency.

## Materials and Methods

**Chronic reduction of cerebral blood flow:** 2VO and sham surgery was performed on male Sprague-Dawley retired breeders (Charles River Laboratories, PQ), 9–10 months of age ( $n = 20$ ) as described in detail previously.<sup>8</sup> Briefly, rats were anesthetized with ketamine (100 mg/kg, i.m.) and sodium methohexital (50 mg/kg, i.p.). A ventral midline incision was made to expose both carotid arteries. The arteries were gently isolated from the carotid sheath and vagus nerve. In 2VO surgery, each carotid artery was double-ligated with 5-0 silk suture just below the carotid bifurcation. In sham operations, the arteries were exposed but not ligated. Rats were closely monitored during post-operative recovery. Two and 27 weeks after surgery animals were deeply anesthetized with sodium pentobarbital and euthanized by cardiac perfusion with heparinized saline followed by 4% paraformaldehyde in 100 mM phosphate buffer (pH 7.4). Brains were post-fixed in phosphate-buffered 4% paraformaldehyde for 24 h at 4°C and paraffin-embedded according to standard histological procedure. Serial coronal sections were cut at 4  $\mu$ m and 14  $\mu$ m. Sections located at -3.3 to -4.3 from bregma were analyzed. All manipulations were performed in compliance with approved institutional protocols and according to the strict ethical guidelines for animal experimentation established by the Medical Research Council (Canada).

**In situ detection and quantitation of apoptotic neurons:** Both histological and biochemical criteria were used to identify apoptotic neurons. Serial sections were processed for hematoxylin and eosin (H/E) staining, Palmgren silver impregnation, and terminal deoxynucleotidyl transferase (TdT)-mediated dUTP nick end labelling (TUNEL) of DNA strand breaks. H/E staining was performed to identify degenerating regions in the dorsal hippocampus. Pyknotic cells exhibiting multiple eosinophilic inclusions with amorphous or fragmented nuclei were defined as apoptotic. Healthy cells had oval nuclei, prominent nucleoli, and lacked eosinophilic cytoplasm. Neurons exhibiting abnormal H/E staining were counted bilaterally at  $\times 250$  magnification by light microscopy. Counts were averaged across both hemispheres to yield a single value for each rat. Palmgren silver impregnation was used to confirm changes in nuclear morphology associated with apoptosis. Nuclei exhibiting membrane blebbing, fragmentation, and hyperchromatic staining were defined as apoptotic. Healthy nuclei were round and homogeneously stained. The total number of CA1 pyramidal neurons were counted in each hemisphere across three serial Palmgren-stained sections

and averaged to yield a single parameter per rat. TUNEL reaction was performed to quantitate cells undergoing DNA fragmentation. Briefly, sections were permeabilized by a 20 min incubation at room temperature in 0.1% Triton X/0.1% sodium citrate, washed in 10 mM PBS pH 7.2, reacted for 1 h at 37°C with TdT and digitonin-labeled dUTP in 30 mM Tris-HCl, pH 7.2, 140 mM sodium cacodylate, 1 mM cobalt chloride, and visualized using an anti-DIG FITC antibody (1:100; Oncor, MD). Sections were coverslipped under glycerol containing 0.1% *p*-phenylenediamine (Sigma) and the number of immunofluorescent TUNEL-positive neurons were counted. Apoptotic glia were not quantified. Because TUNEL can detect both single (DNA repair and early-stage apoptosis) and double strand breaks (apoptosis and late-stage necrosis), labeled neurons were included only if located at sites exhibiting histological evidence of apoptotic death. Thus, cell counts represent the most conservative estimate possible of neuronal apoptosis. Following quantitation, sections were incubated with an anti-FITC peroxidase antibody (1:100; Boehringer Mannheim, PQ) and processed colorimetrically to assess nuclear morphology. Negative controls included sections incubated with DIG-labeled dUTP in the absence of TdT.

**Behavioral assessment:** Rats assigned to the 27 week 2VO- and sham-operated groups ( $n = 5$ /condition) were assessed on five occasions after surgery for radial arm maze performance at 1, 3, 9, 15 and 24 week intervals and for Morris water maze performance at 2, 4, 10, 16, and 25 week intervals. Test apparatuses and testing protocols have been described in detail previously.<sup>12,13</sup> Briefly, in the radial arm maze task, animals were permitted to forage for sucrose reward placed in wells located at the end of a 12 arm maze. Six arms were baited in a quasi-random placement pattern that remained constant across all of the test sessions. The remaining six arms were never baited. Animals were scored for the number of repeat entries into baited arms (working memory errors) and for the total number of entries into unbaited arms (reference memory errors).<sup>14</sup> The mean number of working and reference memory errors were calculated across all of the test trials to establish a single statistic per animal at time of sacrifice.<sup>8</sup> In the Morris water maze task, animals were required to swim towards and mount a hidden platform submerged in opaque water. The platform was located in the same position in the pool on every test session. A single mean overall latency time for location of the platform was calculated per animal by averaging over the 12 trials at each test date.<sup>8</sup>

## Results

*Evidence of apoptosis 2 weeks after 2VO surgery:* Morphological indications of both apoptotic and necrotic cell death were observed 2 weeks post-operative in 2VO rats but not in sham-operated animals. Pyknotic H/E-stained neurons with eosinophilic inclusions and amorphous nuclei characteristic of apoptosis were noted in CA1, CA3b and CA3c pyramidal cell layers of the dorsal hippocampus. Putative apoptotic neurons were often observed in small groups of cells surrounded by glia (Fig. 1A). Less frequently, pyramidal neurons with dense, ubiquitous eosinophilic staining of cell cytoplasm and hyperchromatic hemotoxylin-impregnated nuclei characteristic of necrosis were identified (data not shown). Pyramidal cells in control sections had normal morphology, lacked eosinophilic cytoplasm, and exhibited oval nuclei and prominent nucleoli (Fig. 1C). Rarely, apoptotic morphology was detected in discrete cells in sham-operated subjects (< 2 per dorsal hippocampus). Dying neurons in these control rats were never found in groups, were not surrounded by glia, and could not be consistently localized to specific regions of the hippocampal formation across animals.

Analysis of nuclear morphology provided additional confirmation of apoptosis following 2VO. Palmgren silver impregnation revealed groups of hyperchromatic and amorphous nuclei in CA1, CA3b and CA3c cell fields (Fig. 1D). Often small nuclei characteristic of glia could be observed surrounding the densely stained nuclear fragments. In sham-operated animals, pyramidal cell nuclei were round and homogeneously stained (Fig. 1F).

TUNEL was used to identify DNA strand breaks *in situ*. TUNEL-positive neurons were consistently detected in all of the 2VO animals ( $n = 5$ ), particularly in CA1 and CA3 pyramidal cells, hippocampal interneurons and granule cells of the dentate gyrus (Fig. 2A). The total number of TUNEL-positive neurons per dorsal hippocampus of 2VO animals ( $7 \pm 1.75$ , mean  $\pm$  s.e.m.) was significantly greater than that observed in sham rats ( $0.3 \pm 0.2$ ;  $p < 0.05$ , Student's *t*-test). Cell counts were performed on immunofluorescent cells labelled with DIG-conjugated dUTPs and visualized with an anti-DIG-FITC secondary antibody (Fig. 1G).

Following quantitation, sections were processed colorimetrically using an anti-FITC peroxidase-tagged antibody to more closely examine nuclear morphology (Fig. 1G, inset). This tertiary enhancement provided additional information on the nature of 2VO-induced DNA damage. Substantially more TUNEL-positive pyramidal neurons were detected in 2 week 2VO sections following tertiary reaction

(Fig. 2B). Close examination of morphology indicated that cells that failed to exhibit detectable FITC label prior to tertiary enhancement were not morphologically abnormal (Fig. 1G, inset). Labeling was not, however, artifactual in that not every pyramidal cell was TUNEL-positive following colorimetric processing and no additional labeling was detected in sham-operated animals or at later time points following 2VO surgery (Figs 1H,I,2B).

*Cell loss is accelerated 27 weeks after 2VO surgery:* The number of TUNEL-positive fluorescent neurons in CA3 was significantly increased 27 weeks after 2VO surgery over that detected in sham-operated animals and 2 week 2VO subjects (Fig. 2A). Fewer interneurons in oriens layer, stratum radiatum and lacunosum moleculare layer exhibited TUNEL reactivity (Fig. 2A).

Two qualitative differences in DNA damage were noted. First, TUNEL-positive neurons were not clustered in groups as they had been at 2 weeks but were dispersed as discrete cells (Fig. 1B). While this localization was reminiscent of the infrequent distribution of apoptotic neurons in control tissue, dying 2VO cells were consistently surrounded by glia and were localized to pyramidal cell layers unlike the rate of apoptotic neurons detected in sham-operated subjects (Fig. 1B,E). Second, colorimetric enhancement of TUNEL-processed sections failed to reveal any additional labeling (Fig. 1H). These data confirm that *de novo* detection of low level DNA strand breaks is only evident in 2 week 2VO animals.

Because a neuron, once committed to cell death, can take anywhere from 20 min to several hours to exhibit DNA strand breaks or morphological changes, TUNEL quantitates only those cells well-progressed through an apoptotic program at the exact moment of sacrifice. To establish the relevancy of these data to hippocampal integrity, cell counts of Palmgren-stained sections were performed. In keeping with the rate of apoptosis observed at 2 and 27 weeks following 2VO (Fig. 2A), a significant overall reduction in CA1 (sham  $559 \pm 11$ ; 2VO  $448 \pm 16$ ;  $p < 0.01$ , Student's *t*-test) and CA3c (sham  $112 \pm 7$ ; 2VO  $98 \pm 5$ ;  $p < 0.05$ , Student's *t*-test) pyramidal cell number was detected by 27 weeks post-surgery.

*Behavioral impairment correlates with apoptosis in CA1 pyramidal neurons:* To assess the importance of hippocampal damage on behavior, we correlated performance in radial arm maze and Morris water maze tests with hippocampal apoptosis. A significant correlation was observed between the number of TUNEL-positive neurons observed in the hippocampus 27 weeks post-operative and the number of radial arm maze reference memory errors ( $r = 0.66$ ,

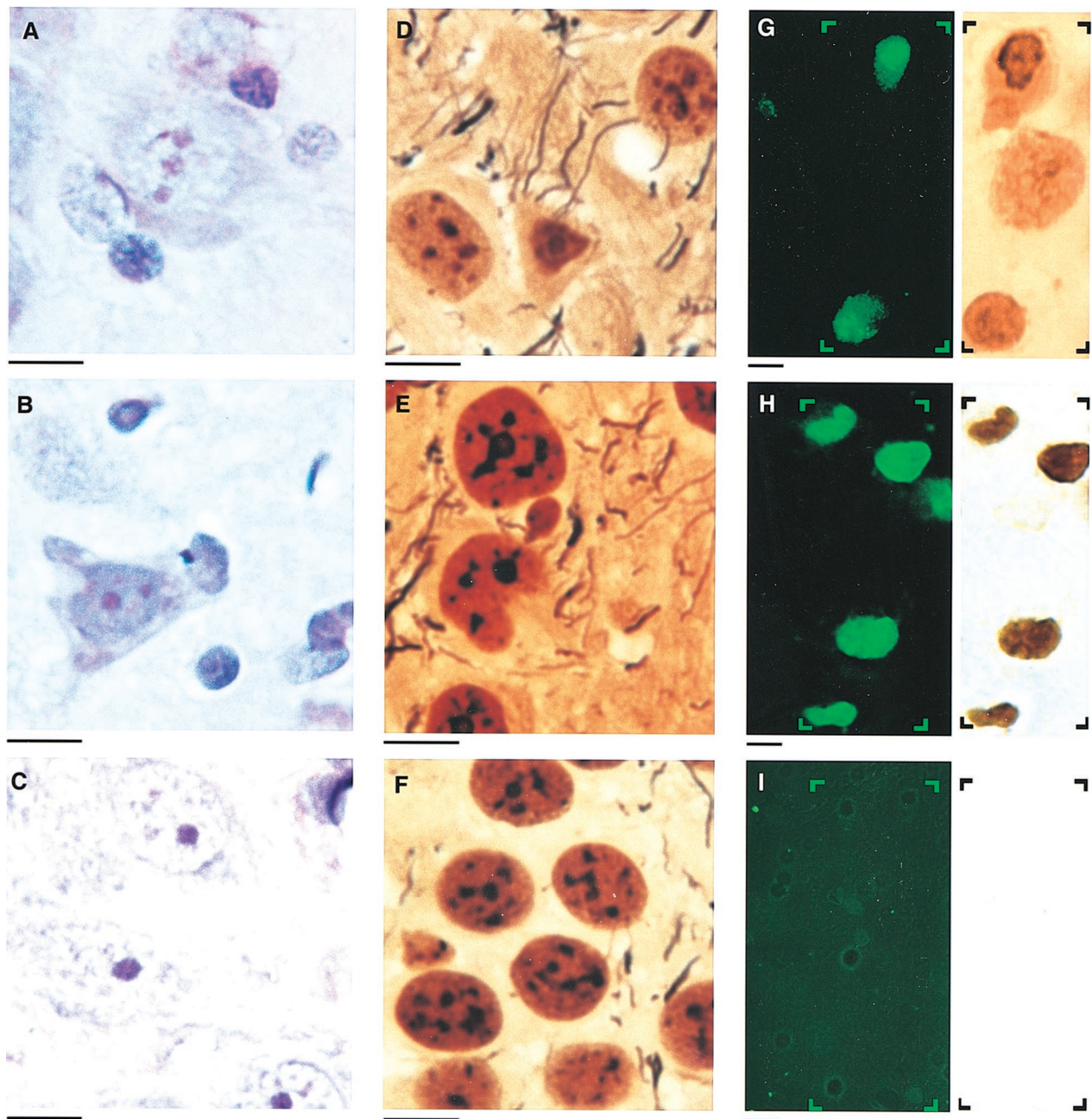


FIG. 1. Histological and biochemical evidence of 2VO-induced apoptosis. Representative photomicrographs of the CA3c region of the hippocampus (A–C) H/E staining. (D–F) Palmgren silver nuclear impregnation. (G–I) TUNEL detection of DNA strand breaks. TUNEL insets depict the same section after tertiary enhancement. Details as in Materials and Methods. Bar = 10  $\mu$ m. Two weeks after 2-VO surgery: (A) Multiple damaged neurons surrounded by glia. (D) Pyknotic Palmgren nuclear staining is observed in a single neuron. Healthy cells are noted on either side. (G) TUNEL reactive neurons. Note the additional TUNEL-positive neighbouring cells with apparent normal nuclear morphology following tertiary enhancement (inset). Twenty-seven weeks after 2VO surgery: (B) A single neuron exhibiting eosinophilic inclusions and nuclear and cytoplasmic blebbing is surrounded by reactive glia apparently involved in phagocytosis. (E) Blebbed Palmgren nuclear morphology. (H) Multiple TUNEL reactive-neurons. Note that additional evidence of DNA damage is not detected in neighbouring cells following tertiary enhancement (inset). Two weeks post-sham surgery: (C) Normal nuclear and cytoplasmic morphology in neurons exhibiting oval nuclei and prominent nucleoli. (F) Round homogeneous silver impregnation of healthy neurons. One small glial nucleus can be seen in this field. (I) No TUNEL reactive pyramidal cells were detected in the hippocampus of sham-operated animals at any time point (inset). Identical results were obtained in sham-operated animals 27 weeks post surgery.

$p < 0.05$ ). Furthermore, the number of reference memory errors correlated significantly with the degree of apoptotic CA1 cells ( $r = 0.86$ ,  $p < 0.01$ ) but not with the number of TUNEL-positive CA3

neurons ( $r = 0.39$ ,  $p > 0.5$ ). Animals that exhibited a higher CA1 to CA3 ratio of TUNEL-positive cells made more reference memory errors than animals with lower CA1 to CA3 ratios ( $r = 0.75$ ). Working

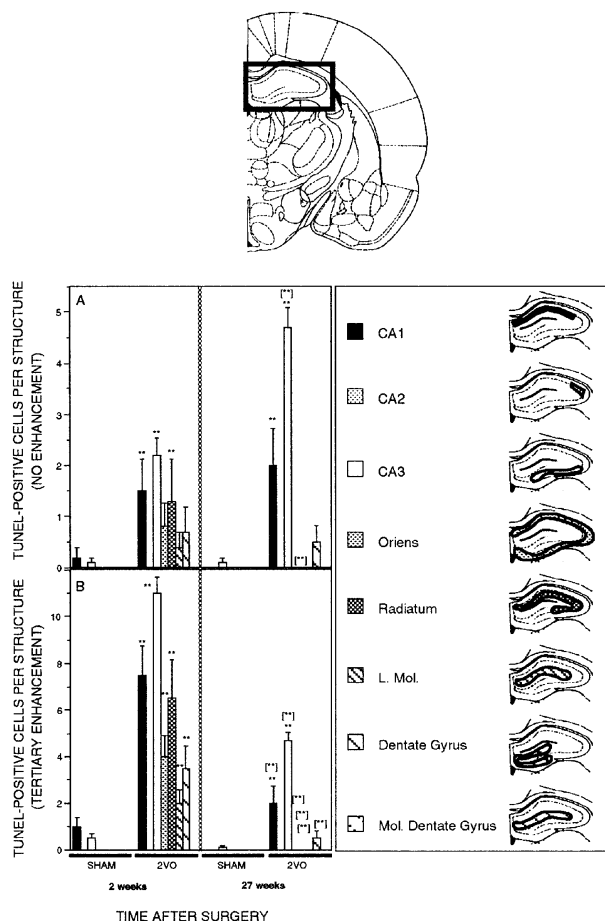


FIG. 2. Quantitation of apoptotic cell loss and DNA damage following 2VO. Data represent the number of TUNEL-positive neurons in each hippocampal region. \*\*Significant difference between 2VO and sham-operated animals (ANOVA, *a priori* contrast of means,  $p < 0.01$ ). [\*] Significant difference between 2VO animals at 2 and 27 weeks (ANOVA, *a priori* contrast of means,  $p < 0.05$  [\*\*]  $p < 0.01$ ). The legend defines the structure in which apoptotic cells were quantitated. (A) Number of immunofluorescent TUNEL-positive cells exhibiting double strand breaks in the dorsal hippocampus. A significant increase in TUNEL was observed in CA1, CA3 and radialium neurons and in CA1 and CA3 neurons at 2 and 27 weeks post-surgery, respectively, compared with sham-operated animals. The number of CA3 neurons exhibiting DNA strand breaks was significantly greater at 27 weeks than at 2 weeks. (B) Number of cells exhibiting single and double-strand breaks detected by tertiary enhancement of TUNEL. A significant number of single strand breaks was only detected 2 weeks post-surgery.

memory errors also significantly correlated with CA1 apoptosis ( $r = 0.65$ ,  $p < 0.01$ ) and animals with a higher CA1:CA3 apoptotic ratio demonstrated more working memory errors than other rats ( $r = 0.66$ ,  $p < 0.01$ ). No correlation was found between hippocampal apoptosis and Morris water maze performance ( $r = 0.36$ ,  $p > 0.05$ ).

## Discussion

Sustained 2VO reduction of cerebral blood flow models the clinical condition of cerebrovascular

insufficiency associated with aging in humans and exacerbated during AD.<sup>1-5</sup> It should be noted that this model is distinct from experimental paradigms of transient global ischemia. In transient ischemic models, a complete reduction of cerebral blood flow is acutely induced for 5–30 min and is followed by a prolonged period of vascular reperfusion. This insult results in an abrupt loss of hippocampal CA1 neurons 1–10 days after surgical intervention and immediate neurological impairment.<sup>15,16</sup> Neuronal apoptosis at later time points has not been reported. By contrast, 2VO animals do not demonstrate acute behavioral dysfunction and survive for at least 12 months without any gross neurological symptoms.<sup>6-8</sup> Rather, 2VO elicits progressive cerebral deterioration manifested in late-emerging CA1 cell loss and apparent memory dysfunction.<sup>8</sup> This paradigm is suited to analyzing damage associated with chronic dementia resulting from prolonged cerebrovascular insufficiency and not to impairment elicited by acute ischemic attack.

In the present study, we provide evidence that chronic reduction of cerebral blood flow induces apoptosis in hippocampal pyramidal neurons. Apoptotic morphology can be identified by pyknosis, multiple eosinophilic inclusions, blebbed or fragmented hyperchromatic nuclei, and *in situ* labeling of DNA strand breaks. Apoptotic neurons were observed at both 2 weeks and 27 weeks after 2VO surgery with an increase in the rate of apoptosis noted at the later time point. The relevancy of this finding is underlined by the decrease in total number of pyramidal cells observed at 27 weeks after 2VO compared with that in sham-operated rats. We have previously demonstrated that this reduction in cell number is not observed at earlier time points.<sup>8</sup> These data suggest that hippocampal damage following 2VO is likely the result of progressive apoptotic cell loss. To our knowledge, this is the first demonstration that a sustained increase in the rate of neuronal apoptosis, elicited by a moderate but chronic cerebral insult, results in a significant reduction in cell number.

We also demonstrate that hippocampal apoptosis following 2VO is accompanied by deteriorating performance on visuospatial memory tasks. The strong correlation between the number of apoptotic cells identified *in situ* and radial arm maze impairment raises the intriguing possibility that cognitive deterioration, associated clinically with chronic cerebrovascular insufficiency, is mediated by apoptotic cell loss. Our data suggest that the type of memory impairment may be determined by location of neuronal cell loss. For example, reference and working memory errors in the radial arm maze are strongly correlated with CA1 not CA3 apoptosis and are most evident when the ratio of CA1 to CA3 cell death is

high. Morris water maze performance is not correlated with hippocampal pathology.

While we have yet to identify the stimulus that triggers apoptosis during chronic hypoperfusion, morphological evidence suggests at least two different types of neuropathology (acute and chronic) although the intermediate kinetics remain undefined. Two weeks post-surgery small groups of apoptotic neurons are observed clustered throughout pyramidal cell layers and interneurons of the hippocampus. *De novo* single strand breaks, evident by tertiary enhancement of TdT-mediated incorporation of labeled nucleic acid, are detected in multiple pyramidal neurons indicative of either early stage apoptosis, prior to cell fate commitment, or DNA repair. This phenotype is reminiscent of the damage elicited in *in vitro* models of acute hypoxic insult and in *in vivo* models of ischemia, in which DNA damage and neuronal death are mediated by sustained depolarization and glutamate excitotoxicity triggered by acute reduction in oxygen.<sup>16–20</sup> At 27 weeks post-surgery, dying neurons are restricted to CA1 and CA3 pyramidal layers and are not detected in groups. This phenotype is reminiscent of cell death observed in *in vitro* models of chronic hypoxia and has been attributed to reduced cerebral mitochondrial respiration resulting in intracellular accumulation of reactive oxygen species.<sup>21,22</sup> We hypothesize that progressive mitochondrial failure may mediate apoptosis in the later stages of 2VO. While this hypothesis is only speculative, we have previously correlated chronic reductions in mitochondrial activity and ADP/ATP conversion with oxidative stress and apoptosis in the regressing rat ventral prostate (unpublished data). It remains to be determined whether a similar event occurs in brain but if this hypothesis proves accurate it predicts that oxyradical

scavengers, increasingly indicated in the treatment of acute ischemic insult, may also prove beneficial in advanced cases of cerebrovascular insufficiency.

## Conclusion

A moderate reduction of cerebral blood flow elicits both acute and chronic increases in apoptotic death in neurons of the rat hippocampus. The degree of apoptotic cell loss correlates with behavioral impairment. These data provide the first indication that sustained neuronal apoptosis may underlie progressive cognitive failure associated with clinical conditions of chronic cerebrovascular insufficiency.

## References

1. Barrow DL. *Neurosurgery* **23**, 484–490 (1988).
2. de la Torre JC and Mussivand T. *Neurol Res* **15**, 146–153 (1993).
3. Schmidt-Kastner R, Fliss H and Hakim AH. *Stroke* **28**, 163–170 (1997).
4. Sekhon LHS, Morgan MK, Spence I et al. *Neurosurgery* **40**, 548–556 (1997).
5. Kalaria RN and Hedera P. *Neuroreport* **6**, 477–480 (1995).
6. de la Torre JC, Fortin T, Park GAS et al. *Brain Res* **623**, 6–15 (1993).
7. de la Torre JC, Fortin T, Park GAS et al. *Brain Res* **582**, 186–195 (1992).
8. Pappas BA, de la Torre JC Davidson CM et al. *Brain Res* **708**, 50–58 (1996).
9. Kerr JFR, Wyllie AH and Currie AR. *Br J Cancer* **26**, 239–257 (1972).
10. Wyllie AH, Kerr JFR and Currie AR. *Int Rev Cytol* **68**, 251–306 (1980).
11. Tenniswood M, Guenette RS, Lakins J et al. *Cancer Metastasis Rev* **11**, 197–220 (1992).
12. Murtha SJE and Pappas BA. *Brain Res* **651**, 16–26 (1994).
13. Park GAS, Pappas BA Murtha SM et al. *Neurosci Lett* **143**, 259–262 (1992).
14. Olton DS and Pappas BC. *Neuropsychologia* **17**, 669–682 (1979).
15. MacManus JP, Buchan AM, Hill IE et al. *Neurosci Lett* **164**, 89–92 (1993).
16. Nitatori T, Sato N, Waguri S et al. *Neurosci* **15**, 1001–1011 (1995).
17. Haddad GG and Donnelly DF. *Physiol* **429**, 411–428 (1990).
18. Heron A, Pollard H, Dessi F et al. *J Neurochem* **61**, 1973–1976 (1993).
19. Ikeda J, Terakawa S, Murota S et al. *J Neurosci Res* **43**, 613–622 (1996).
20. Rothman SM. *Science* **4596**, 536–537 (1983).
21. Ankarcona M, Dypbukt JM, Bonfoco E et al. *Neuron* **15**, 961–973 (1995).
22. Chavez JC, Pichiule P, Boero J et al. *Neuroscience Letters* **193**, 169–172 (1995).

ACKNOWLEDGMENTS: This work was funded by grants from the Alzheimer Society of Canada to S.A.L.B., the National Institute of Health (USA) #CA69233 to M.P.R.T., and the Ontario Heart and Stroke Foundation (Canada) to B.A.P. The authors would like to thank J. Bennett for critical and technical assistance.

Received 21 October 1997;  
accepted 14 November 1997